

THERMOPHYSICAL PROPERTIES MAPPING IN SEMI-INFINITE LONGITUDINALLY CRACKED PLATES BY TEMPERATURE IMAGE PROCESSING

Olivier Fudym, Roberto Santander

*Universidad de Santiago de Chile,
Dpto.Ing.Mecánica, Av.Lib.Bdo. O'Higgins 3363,
Casil. 10233, Santiago, Chile
ofudym@lauca.usach.cl*

J.-Christophe Batsale, J.-Luc Battaglia

*Université de Bordeaux 1
TREFLE, ENSAM, Esp. des Arts et Métiers,
33405 Talence cedex, France
batsale@lept-ensam.u-bordeaux.fr*

ABSTRACT

Thermophysical properties mapping in a solid plate from transient temperature imaging analysis is widely developed. Most usual methods are based on very restrictive assumptions such as the independence of the pixels (one dimensional diffusion with uniform heating of the front face of the sample). One difficulty is to take into account the spatial correlation between pixels due to 3D transverse effects.

Such correlation is taken into account in specific experimental situations such as the flying spot techniques, where the sample is assumed to be locally homogeneous. Other situations remains difficult because the estimation of thermophysical properties field from 2D temperature measurement is an ill-posed problem. Moreover, the practical implementation of the estimation is here affected by the large amount of the vectors (or matrices) to be observed and estimated.

In order to overcome such problems a semi numerical analysis with a spatially random front face excitation is proposed here to detect a crack mapping with the cracks laid perpendicular to the excitation surface.

INTRODUCTION

Estimating a mapping of thermophysical properties from the analysis of transient images of temperature responses to a given heat excitation is widely developed. It is known as thermal non-destructive evaluation or thermal NDE. It has been largely improved with the rapid evolution of IR cameras and the possibilities of image processing related to such devices.

Detecting delaminations in thin plates of composite materials (or horizontal cracks following the plane direction of the composite plate) by infrared thermography has been studied since 1980 (see for example [1]). The majority of the processing methods associated to delamination detection consists in considering only a 1D heat transfer following the thickness direction, even if 2D or 3D heat transfer corrections have been studied (see [2]). In 1D experiments each pixel of the IR image is then assumed to be independent (non-correlated) of the other neighbouring pixels. In all classical experimental situations the in-plane diffusion effects are avoided with experimental precautions (spatially uniform excitation, thin samples...).

At the opposite, methods based on in-plane diffusion in transient state have been implemented with very restrictive assumptions (homogeneous samples). They allow to estimate the macroscopic thermal diffusivity of anisotropic samples (see [3],[4]) or to study periodic heterogeneity by the consideration of homogenisation methods (see [5]). One of the main difficulties is then to take into account the spatial correlation of the pixels induced by 2D heat transfer. The thermal study of heterogeneous samples has been implemented with a successful technique called the « flying spot » method (see [6]). It consists in moving a laser hot spot on the front face of the sample and analysing the local transient temperature field around the spot. Such a method is efficient but experimentally difficult (slow scanning of the domain, optics and laser techniques, very short characteristic time of diffusion...). Moreover, only the thermally excited domain can be processed and only a few pixels can be concerned.

From a general point of view, estimating a 2D or 3D mapping of thermophysical properties from a 2D transient temperature field, without any assumption about the distribution of the properties, is an « ill-posed » problem. The implementation of general inverse methods presents particular difficulties. In fact, the size of the parameter vector to estimate is great and consequently, the size of the associated Hessian matrices to invert is great too. Then, the quantity of data to minimise is quite huge and at last, there is the problem of the « classical » ill conditioning of the Hessian. The problem has only been studied in stationary state (see [7] for a bibliographic review of such problems). Paradoxically, such a situation is difficult to be experimentally developed because the stationary thermal non-equilibrium needs a lot of difficult precautions (temperature regulations, control of the heat losses...).

The main idea of this work is to propose a new evaluation method, which associates a simple experiment in transient state and some classical considerations about the maximum likelihood principle and estimation theory in linear cases. The aim is to estimate the diffusivity field by processing some successive images in diffusive evolution from a spatially random initial temperature distribution. Inversion of great systems is avoided due to neighbourhood considerations of the heat transfer. The property of thermal diffusion is represented by the Laplacian operator, which correlates the signal of one pixel and its immediate spatial neighbours. The thermal inertia is represented by the time derivative which correlates the signal of one pixel at times t and $t + \Delta t$. It is then possible to process the large amount of data with the same principle as autoregressive methods on spatial fields, while such methods are usually applied to process 1D transient signal (see [8]).

The specific case studied here is related to the estimation of a 2D field of properties from the observation of a 2D transient successive images but in a case of 3D transient diffusion (heat pulse on a fractured semi-infinite sample). Such situation is related to the need of experimental characterization of fractured media in various domains such as composite materials, geological samples, small scale structural analysis of metallic samples.

The advantage of the semi-numerical quadrupole method used here is to consider the separability of the 3D-transient temperature distribution. The forward problem and the estimation method will be presented in the next sections. Numerical examples will then be explained in order to examine the practical aspects of the method.

EXPERIMENTAL SITUATION AND FORWARD PROBLEM

The main objective of the present work is to propose new estimation methods related to simple experiments (see figure 1) in order to estimate cracks cartographies in the particular case where the cracks are perpendicular to the observation surface (x - y surface) and uniform following the z -direction. The experiment consists in making a heat pulse excitation on the front face of a semi-infinite sample, initially uniformly at zero temperature and with lateral adiabatic conditions. A spatially random radiation is obtained with a semitransparent film inserted between the lamp and the samples. After the pulse, the lamp and the film are removed and the front face (x - y surface at $z=0$) temperature field is observed. The main originality of the front excitation is to be spatially random instead of a unique spot or spatially uniform radiation.

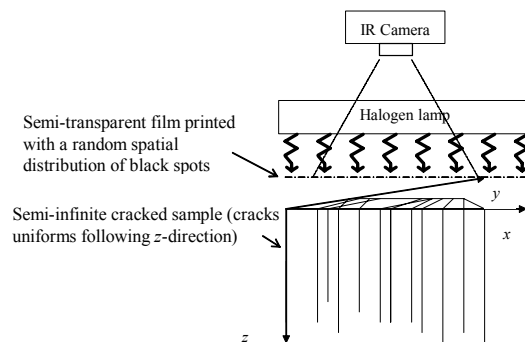


Fig 1: *Scheme of the experimental device*

In a medium with uniform properties versus z -direction and cracks perpendicular to the front surface, such as the one depicted in Figure 1, 3D transient heat diffusion is governed by the following general equation :

$$k_z \frac{\partial^2 T}{\partial z^2} + \frac{\partial}{\partial x} \left(k_x(x,y) \frac{\partial T}{\partial x} \right) + \frac{\partial}{\partial y} \left(k_y(x,y) \frac{\partial T}{\partial y} \right) = \rho c \frac{\partial T}{\partial t} \quad (1)$$

The method is concerned by the detection of cracks, which are thin air layers of low thermal inertia. In such a situation, only a thermal conductivity variation $k_x(x,y)$ and $k_y(x,y)$ of the sample will be considered, while the volumic specific heat ρc and the thermal conductivity k_z will be assumed to be uniform.

At this stage, a semi-analytical quadrupole approach is applied in order to solve such a system (see [9],[10],[11]). Space discretization of expression (1) is performed only versus x and y direction and considered as continuous versus the z direction. The temperature field is then represented by the $N \times N$ nodes i,j defining $T_{i,j}(z,t)$. Performing a Laplace transformation, such as:

$$\bar{T}_{i,j}(z,s) = \int_0^{\infty} \exp(-st) T_{i,j}(z,t) dt \quad (2)$$

Introducing the vector $\bar{\mathbf{T}}$ which components are the Laplace transformed temperatures $\bar{T}_{i,j}(z,s)$ at the position z , expression (1) can be written in such a matrix form:

$$\left(k_z^{-1} \mathbf{M}_{//} + a_z^{-1} s \mathbf{I} \right) \bar{\mathbf{T}} - \frac{d^2 \bar{\mathbf{T}}}{dz^2} = 0 \quad (3)$$

where $\mathbf{M}_{//}$ is a finite differences operator, \mathbf{I} the identity matrix (Matrices of size $N \times N$) and a_z is a constant longitudinal thermal diffusivity such as: $a_z = k_z / \rho c$. The general solution of such ordinary differential system can be presented with a function of matrix such as:

$$\bar{\mathbf{T}}(z,s) = \exp\left(-\left(k_z^{-1} \mathbf{M}_{//} + a_z^{-1} s \mathbf{I}\right)^{1/2} z\right) \bar{\mathbf{T}}(0,s) \quad (4)$$

A direct relationship between the Laplace front face temperature vector $\bar{\mathbf{T}}(z=0,s)$ and the Laplace heat flux vector $\Psi(z=0,s)$ is found for the semi-infinite medium as (see [11]):

$$\bar{\mathbf{T}}(z=0,s) = \mathbf{Z} \Psi(z=0,s) \quad (5-a)$$

\mathbf{Z} is a transfer matrix defined as:

$$\mathbf{Z} = \left(k_z^{-1} \mathbf{M}_{//} + a_z^{-1} s \mathbf{I} \right)^{-1/2} k_z^{-1} \quad (5-b)$$

The function of matrix used in expression (5-b) is here separable by using the shift properties of the Laplace transform. If the longitudinal diffusivity a_z is non-uniform versus x and y , the problem becomes then non separable (see [11]).

Here, $k_z^{-1} \mathbf{M}_{//}$ is diagonalisable such as: $k_z^{-1} \mathbf{M}_{//} = \mathbf{P}(\mathbf{\Omega}) \mathbf{P}^{-1}$ with $\mathbf{\Omega}$ diagonal matrix. It induces that

$$\mathbf{Z} = \mathbf{P} \left(\mathbf{\Omega} + a_z^{-1} s \mathbf{I} \right)^{-1/2} \mathbf{P}^{-1} k_z^{-1} \quad (6)$$

If the excitation on the front face is a heat pulse, the components of vector $\Psi(z=0,s)$ are constant independent on the s variable ($\Psi(z=0,s) = \Psi_0$).

Since elementary properties of inverse Laplace transform are considered such as

$$\begin{aligned} L^{-1}\left(1/\sqrt{s}\right) &= 1/\sqrt{\pi t} \text{ and} \\ L^{-1}\left(1/\sqrt{s+K}\right) &= \exp(-Kt)/\sqrt{\pi t} \end{aligned} \quad (7)$$

From expression (7), the inverse Laplace transform of $\bar{\mathbf{T}}(z=0,s)$ is turned into:

$$\mathbf{T}(z=0,t) = \frac{1}{\sqrt{\pi t / a_z}} \mathbf{P} \exp(-a_z \mathbf{\Omega} t) \mathbf{P}^{-1} k_z^{-1} \Psi_0 \quad (8-a)$$

or with exponential of matrix notation :

$$\mathbf{T}(z=0,t) = \frac{1}{\sqrt{\pi t / a_z}} \exp\left(-(\rho c)^{-1} \mathbf{M}_{//} t\right) k_z^{-1} \Psi_0 \quad (8-b)$$

If the averaged temperature versus x and y direction is considered, such as:

$$\langle T \rangle(z,t) = \frac{1}{N^2} \sum_{i=1}^N \sum_{j=1}^N T_{i,j}(z,t) \quad (8-c)$$

The behaviour of $\langle T \rangle(z,t)$ is then only related to the first eigenvalue of matrix $\mathbf{M}_{//}$ which is zero, such as :

$$\langle T \rangle(z=0,t) = \frac{1}{\sqrt{k_z \rho c \pi t}} \frac{1}{N^2} \sum_{i=1}^N \sum_{j=1}^N \Psi_{i,j}(z=0) \quad (8-d)$$

Such situation allows to consider that the temperature response to any heat pulse excitation

at $z=0$ can be expressed as the product of two separated temperature evolutions such as:

$$T_{x,y,z}(x, y, z, t) = T_{x,y}(x, y, t) \times T_z(z, t) \quad (9)$$

At $z=0$, the previous expression becomes:

$$\begin{aligned} T(x, y, z=0, t) \\ &= T_{x,y}(x, y, t) \times T_z(z=0, t) \\ &= T_{x,y}(x, y, t) \times C / \sqrt{t} \end{aligned} \quad (10)$$

At this stage, only a constant C is considered in expression (10) instead of the exact proportionality coefficient for exact temperature level, because exact IR temperature measurements are very difficult (knowledge of emissivity, detectors calibration). Such proportionality coefficient will not be taken into account in the next steps, but does not disturb the diffusivity estimation procedure.

The analysis of the observable $T_{x,y}(x, y, t) = T_{x,y,z}(x, y, z=0, t) \times \sqrt{t}$ is then related to the analysis of a purely 2D signal which verify a 2D diffusion problem such as:

$$\rho c \frac{\partial T_{x,y}}{\partial t} = \frac{\partial}{\partial x} \left(k_x(x,y) \frac{\partial T_{x,y}}{\partial x} \right) + \frac{\partial}{\partial y} \left(k_y(x,y) \frac{\partial T_{x,y}}{\partial y} \right) \quad (11)$$

IMPLEMENTATION OF THE ESTIMATION METHOD

At this stage, for easier presentation, the discretized vector related to the transformed 2D field: $T_{x,y,z}(x, y, z=0, t) \times \sqrt{t}$ is noted: \mathbf{T}^t .

The estimation problem is then reduced to a 2D heat transfer problem and previous matrix notation (expression 8-b) allows to write:

$$\mathbf{T}^{t+\Delta t} = \exp(-(\rho c)^{-1} \mathbf{M}_{//} \Delta t) \mathbf{T}^t \quad (12a)$$

For small time step, it yields the following classical explicit expansion:

$$\mathbf{T}^{t+\Delta t} \approx \mathbf{T}^t - (\rho c)^{-1} \Delta t \mathbf{M}_{//} \mathbf{T}^t \quad (12b)$$

The decomposition of the finite differences matrix $\mathbf{M}_{//}$ yields then:

$$\mathbf{T}^{t+\Delta t} - \mathbf{T}^t = \mathbf{A} \cdot \Delta \mathbf{T}^t + \delta_x \mathbf{A} \cdot \delta_x \mathbf{T}^t + \delta_y \mathbf{A} \cdot \delta_y \mathbf{T}^t \quad (13)$$

The notation « \cdot » represents term to term multiplication between vectors, such as in Matlab software notations (see www.mathworks.com).

with:

$$\mathbf{T}^t = [T_{i,j}^t]; \Delta \mathbf{T}^t = [T_{i+1,j}^t + T_{i-1,j}^t + T_{i,j+1}^t + T_{i,j-1}^t - 4 \cdot T_{i,j}^t] \quad (14a)$$

$\Delta \mathbf{T}^t$ is a vector obtained by the Laplacian of the previous vector \mathbf{T}^t .

$$\begin{aligned} \delta_x \mathbf{T}^t &= [T_{i+1,j}^t - T_{i-1,j}^t] \\ \delta_y \mathbf{T}^t &= [T_{i,j+1}^t - T_{i,j-1}^t] \end{aligned} \quad (14b)$$

$\delta_x \mathbf{T}^t$ and $\delta_y \mathbf{T}^t$ are vectors obtained with spatial shifts and differences of the vector \mathbf{T}^t .

$$\mathbf{A} = \frac{\Delta t}{\Delta x^2 \rho c} [k_{i,j}] = \frac{\Delta t}{\Delta x^2} [a_{i,j}]$$

$$\delta_x \mathbf{A} = \frac{\Delta t}{\Delta x^2 \rho c} [k_{i+1,j} - k_{i-1,j}];$$

$$\delta_y \mathbf{A} = \frac{\Delta t}{\Delta x^2 \rho c} [k_{i,j+1} - k_{i,j-1}] \quad (15)$$

\mathbf{A} , $\delta_x \mathbf{A}$, and $\delta_y \mathbf{A}$ are vectors related to the local diffusivities which are parameters of the system, they are obtained with spatial shifts and differences of the previous vector \mathbf{A} . The lateral faces are assumed to be adiabatic.

From expression (13) the temperature mapping $\mathbf{T}^{t+\Delta t}$ is easily calculated at time $t + \Delta t$ from the knowledge of temperature mapping \mathbf{T}^t at time t . Such an approximation is only valid if time and space steps Δt and Δx are small. One other criterion such as: $4a_{i,j} \Delta t / \Delta x^2 \ll 1$ must be verified at each node (see [12]) from the temperature image is assumed to be uniform and non-dependent from the pixels in the neighbourhood. Since the measured temperature of the pixel is multiplied by \sqrt{t} , the covariance matrix related to propagation of the measurement noise on the $\mathbf{T}^{t+\Delta t} - \mathbf{T}^t$ is proportional to t .

The estimation of a parameter vector \mathbf{B} composed of the vectors \mathbf{A} , $\delta_x \mathbf{A}$ and $\delta_y \mathbf{A}$ can then be obtained by considering the minimization of the ponderated quadratic distance S such as:

$$S = \left((\hat{\mathbf{T}}' - \hat{\mathbf{T}}) - \mathbf{X}\mathbf{B} \right)^T \mathbf{t}^{-1} \left((\hat{\mathbf{T}}' - \hat{\mathbf{T}}) - \mathbf{X}\mathbf{B} \right) \quad (16)$$

where $(\hat{\mathbf{T}}' - \hat{\mathbf{T}})$ is an observable vector whose components are the difference between successive temperature images observed at time t and $t + \Delta t$ and \mathbf{X} is a rectangular sensitivity matrix whose components are linear combinations such as:

$$\hat{\mathbf{T}}' - \hat{\mathbf{T}} = \begin{bmatrix} \hat{\mathbf{T}}^{t_0 + \Delta t} - \hat{\mathbf{T}}^{t_0} \\ \cdot \\ \hat{\mathbf{T}}^{t_k + \Delta t} - \hat{\mathbf{T}}^{t_k} \\ \cdot \end{bmatrix}$$

$$\mathbf{X} = \begin{bmatrix} \Delta \hat{\mathbf{T}}^{t_0} & \delta_x \hat{\mathbf{T}}^{t_0} & \delta_y \hat{\mathbf{T}}^{t_0} \\ \cdot & \cdot & \cdot \\ \Delta \hat{\mathbf{T}}^{t_k} & \delta_x \hat{\mathbf{T}}^{t_k} & \delta_y \hat{\mathbf{T}}^{t_k} \\ \cdot & \cdot & \cdot \end{bmatrix}; \quad \mathbf{B} = \begin{bmatrix} \mathbf{A} \\ \delta_x \mathbf{A} \\ \delta_y \mathbf{A} \end{bmatrix}$$

and $\mathbf{t} = \text{diag}[t_0 \dots t_k \dots]$

(17)

One estimator of the parameter vector \mathbf{B} yields from the maximum likelihood principle (see [13]):

$$\mathbf{B} = \left(\mathbf{X}^T \mathbf{t}^{-1} \mathbf{X} \right)^{-1} \mathbf{X}^T \mathbf{t}^{-1} (\hat{\mathbf{T}}' - \hat{\mathbf{T}}) \quad (18)$$

The main advantage of Eq. (18) is that $\mathbf{X}^T \mathbf{t}^{-1} (\hat{\mathbf{T}}' - \hat{\mathbf{T}})$ is a weighted sum of the signal which can be incremented in real time without memory storage. Even if the signal is noisy, the great deal of data (observable vector $\hat{\mathbf{T}}' - \hat{\mathbf{T}}$) can allow a very confident estimation of \mathbf{B} . The inversion of $(\mathbf{X}^T \mathbf{t}^{-1} \mathbf{X})$ is reduced to the inversion of successive small sized (3x3) matrices which can be implemented with symbolic computation softwares (see the "symbolic math toolbox" of Matlab, (www.mathworks.com)).

It is important to note that the main difficulty of the general problem linked to the estimation and handling of great parameter vector and systems is here avoided. For the sake of simplicity, the ill conditioning problems of $(\mathbf{X}^T \mathbf{t}^{-1} \mathbf{X})$ and other problems due to the fact that \mathbf{X} is built from the observable will not be considered here.

In the case of low cost cameras with very noisy signal, the main objective is to develop

rough but simple evaluation methods instead of very accurate but difficult estimation methods from expression (18), with a small number of parameters.

If the parameter vector is reduced to the \mathbf{A} matrix, the sensitivity matrix \mathbf{X} becomes:

$$\mathbf{X} = \begin{bmatrix} \Delta \hat{\mathbf{T}}^{t_0} \\ \cdot \\ \Delta \hat{\mathbf{T}}^{t_k} \\ \cdot \end{bmatrix} \quad (19)$$

The inversion of $\mathbf{X}^T \mathbf{t}^{-1} \mathbf{X}$ is then easy and the estimation is reduced to:

$$\mathbf{A} = \left(\left[\Delta \hat{\mathbf{T}} \right]^T \mathbf{t}^{-1} \left[\Delta \hat{\mathbf{T}} \right] \right)^{-1} \left[\Delta \hat{\mathbf{T}} \right]^T \mathbf{t}^{-1} (\hat{\mathbf{T}}' - \hat{\mathbf{T}}) \quad (20)$$

Equation (20) is a biased expression since it is only deduced from a first order approximation of the system (13). Nevertheless, such an approximation allows to understand and to improve the experimental conditions.

The very simple structure of the sensitivity matrix presented in expression (20) allows to deduce that the best estimation conditions will occur when the Laplacian of the temperature image $\Delta \hat{\mathbf{T}}$ is maximum. Of course, the relaxation of the temperature field due to the diffusion process will be minimum or zero at long time and maximum at the initial state. Thus, a uniform temperature field or a linear one in x or y direction is not efficient because its Laplacian is nearly zero in the case of homogeneous sample. The optimal field exists, but it requires a priori knowledge of the mapping of thermal properties, which is precisely the aim of the study. In such situation, a spatially random initial field appears to be the best compromise. It allows to obtain a temperature field with a uniform spatial spectral density at initial time.

SOME NUMERICAL EXAMPLES

In order to allow a simple presentation of different aspects of the method, only 1D images will be calculated by the forward method and then inverted. Nevertheless, all the remarks given here can be extended to the case of 2D images without difficulties.

One example of matlab software is given in appendix, in order to give more details about the practical implementation.

Such examples will help the experimentalist to explore the limitations of the numerical processing and to design the experiment.

It will there consist to solve numerically the forward problem (expression of $\mathbf{T}^{t+\Delta t}$ from the knowledge of \mathbf{T}^t with the explicit system (13). The simulated IR image is then obtained with a division by \sqrt{t} and a random noise addition.

The estimation of the \mathbf{A} matrix is then obtained by a product of the simulated image by \sqrt{t} and processing with expressions (18) or (20).

The parameters introduced in the calculation are very near from experimental conditions in the field of NDE for composite or metallic media ($N=100, a=10^{-4} m^2 s^{-1}, \Delta x=0.005m, \Delta t=0.04s$).

The fractures are represented by lower diffusivity distribution on very limited zones (generally 1 pixel width). Obviously, the fracture will not be precisely located, due to the resolution limitations of the imaging system.

Example 1: Homogeneous plate locally excited

The first example is devoted to the study of a homogeneous plate only locally excited by a heat pulse at $x=0$ and $z=0$. It consists in considering an initial vector: \mathbf{T}^{t_0} as: $\mathbf{T}^{t_0} = [1, 0, 0, 0, \dots]$ in incrementation given by expression (13).

In the case of a homogeneous medium, an analytical expression is available and allows to validate the numerical scheme. Such analytical model can also be linked to the initial temperature field observed at $t=0$ on the front face of the sample.

$$T_x(x,t) = \frac{1}{2\sqrt{\pi t}} \exp\left(-\frac{x^2}{4at}\right) \quad (21)$$

The observation of the temperature field calculated from Eq. (13) allows to locally estimate the diffusivity field which is here homogeneous. The Fig. 2-a shows the temperature distribution at several time steps. The estimation results obtained from Eq. (18) - respectively Eq. (20) are plotted on Fig. 2-b (resp. Fig. 2-c). It can be observed that the estimation is only efficient in a zone where the temperature field is perturbed. The estimation of the theoretical diffusivity is quasi-perfect near $x=0$ and $y=0$ (or $i=j=1$), then, the estimation becomes biased when the temperature gradient is becoming to be low. The constant bias observed out of the excited zone is related to the uncertain

sensitivity matrix. The simpler expression (20) gives here a larger estimated zone than expression (18).

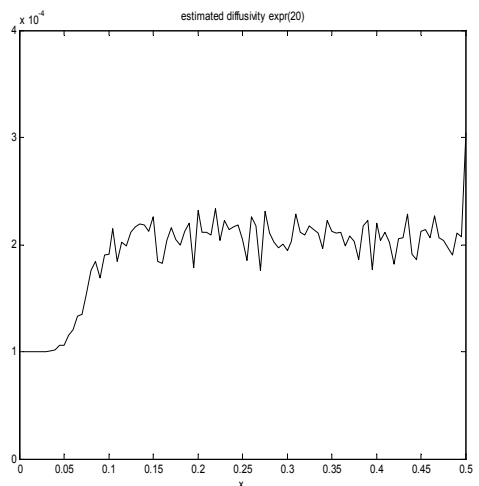
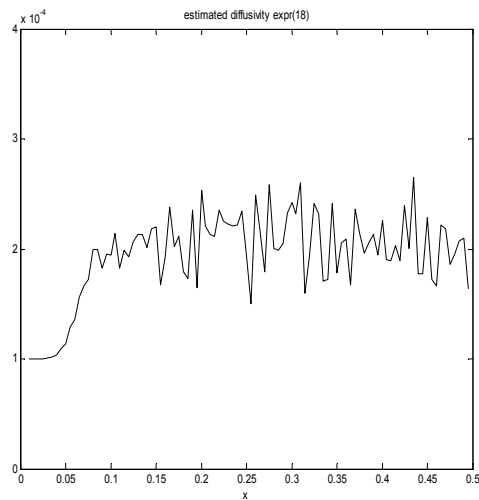
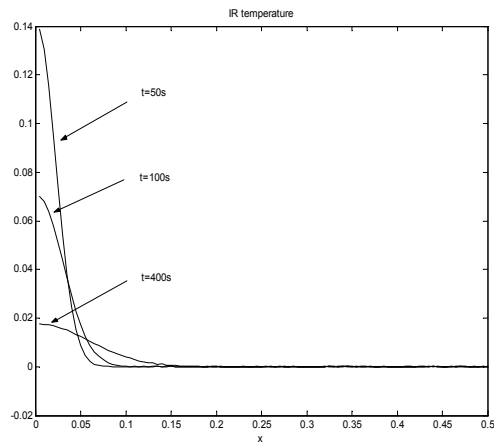


Fig 2: a-several temperature distributions; b- estimated diffusivity distribution with expression (18); c- estimated diffusivity distribution with expression (20). Estimations obtained with 400 time steps and noise amplitude: $\text{sig}=0.0001$ (see the software)

Example 2: Heterogeneous medium, with two defaults and randomly distributed excitation

The energy of excitation is distributed all over the plate. The initial 2D temperature distribution is then such as: $\mathbf{T}^{t_0} = \text{rand}(N,1)$ (“rand” of Matlab, see www.mathworks.com). The sample contains both a thin crack and a larger heterogeneous zone. ($a_{\text{cracks}} = 10^{-5} \text{ m}^2 \text{ s}^{-1}$; $a_{\text{sane}} = 10^{-4} \text{ m}^2 \text{ s}^{-1}$).

The figure 3-a shows then the temperature distributions at several time steps.

The estimation of the diffusivity distribution with Eq.(18) is shown on Fig. 3-b and from Eq. (20) on Fig. 3-c. Equation (18) gives a better resolution but is noisier than Eq. (20) which is a slightly biased in the case of localized defects. Of course, such results could be greatly improved with a lower measurement noise, or a higher initial temperature field.

This example clearly demonstrates the practical advantage of such method compared to a one spot technique (see the previous example). The estimation of the mapping is made instantaneously all over the sample.

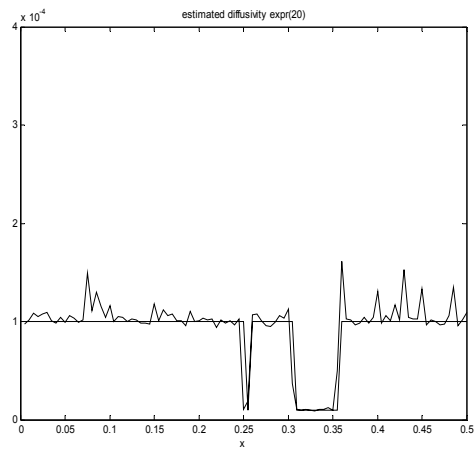
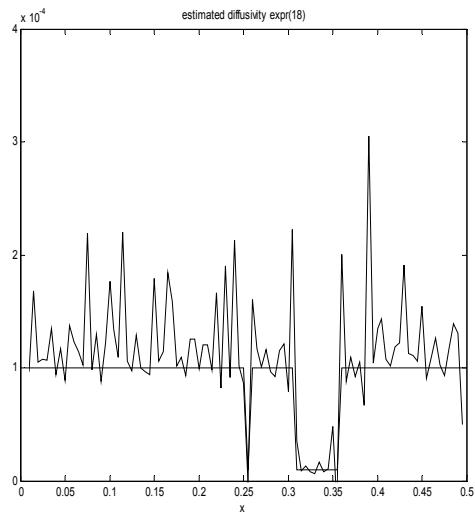
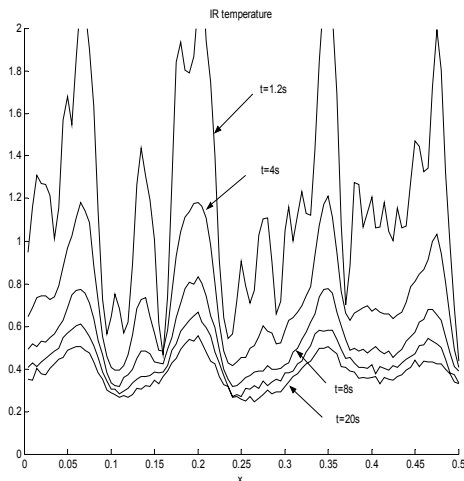


Fig 3: a-Several temperature distributions; b- estimated diffusivity distribution with expression (18); c-estimated diffusivity distribution with expression (20). Estimations obtained with 50 time steps and noise amplitude: $\text{sig}=0.01$ (see the software in appendix)

CONCLUSION

This work is an application of the semi-analytical quadrupole approach ([9],[10],[11]) which is here very helpful to demonstrate the separability of the 3D temperature field. It allows to implement then an efficient inverse method with simple consideration relative to linear estimation methods.

The great advantage of such methods is to avoid memory storage and to offer a simple way to process the great quantity of data related to 3D heat diffusion in heterogeneous media.

Some perspectives are to explore the experimental limits and the bias resulting from the uncertain sensitivity matrix. Some other situations such as time-periodic and space-random excitation or time and space-random are also of interest.

Acknowledgments

The authors gratefully acknowledge the support of the Department of Regional Cooperation in the South Cone and Brasil at the French Embassy in Chile.

REFERENCES

- [1] Balageas D., Delpéch JP, Boscher D, Deom A., *New developments in stimulated infrared thermography applied to non destructive evaluation of laminates*, Review on Progress in Quantitative Non-Destructive Testing, (Plenum Press, New York, (1991) **10 A**, pp 1073-1081.
- [2] Batsale J.C., Maillet D., Degiovanni A., Extension de la méthode des quadripôles thermiques à l'aide de transformations intégrales- Application au défaut plan bidimensionnel, *Int.J.Heat.Mass.Transfer*, (1994,), **37**, n1, pp111
- [3] Philippi I., Batsale JC, Maillet D , Degiovanni A., -Measurement of thermal diffusivity trough processing of infrared images -*Rev. Sci. Instrum.* **66-1**(1995) pp182-192.
- [4] Krapez J.-C., Simultaneous measurement of in-plane and out-of-plane diffusivity by using a grid-like mask, *5th Int. Workshop on Advanced Infrared Techn.*, Venezia (Italy), Sept. 29-30, (1999), E. Grinzato et al. Eds., pp. 289-.
- [5] Varenne M., Batsale J.C., Infrared images processing and volume averaging method in order to estimate 1D or 2D thermal conductivity fields. *Ima. Anal. & Stereologie*, **20-2** sup 1, (2001) 299-
- [6] Gruss C. et Balageas D., (1992), Theoretical and experimental applications of the flying spot camera, (QIRT 92), *Ed Europ Thermique et Industrie*, (1992), pp19-24.
- [7] Jones MR, Tezuda A., Yamada Y, Thermal tomographic detection of inhomogeneities, *J.l of Heat Transfer*, **117**, (1995) pp969-975.
- [8] Jung L., System identification theory for the user, *Prentice Hall ; Englewood Cliffs*. (1987)
- [9] Maillet D., Andre S., Batsale J.C., Degiovanni A. , Moyné C.: Thermal quadripoles- Solving the heat eq. through int. transforms- *Wiley* (2000)
- [10] Fudym O., Ladevie B., Batsale JC., A semi-numerical approach for heat diffusion in heterogeneous media. One extension of the

analytical quadrupole method. *Numerical Heat Transfer.Part B-Fundamentals*, (2002) **42-4** 325–348

- [11] Fudym O., Batsale JC., Lecomte D., Heat diffusion at the boundary of stratified media.Homogenized temperature field and thermal constriction. *Int. J. Heat Mass Transfer*, (2004) **47**, pp 2437-2247
- [12] Ozisik N., Heat Transfer a basic approach, *Mac Graw Hill* (1988)
- [13] Beck J.V., Arnold K.J., Parameter estimation in engineering and science, *Wiley* (1977)

APPENDIX: matlab software (example)

```
%data
N=100;ax=1e-4;dt=0.04;dx=0.005;delt=dt/dx/dx;
x=dx*(1:N); H=[0 N*dx 0 4*ax];sig=0.01; %data
T0=rand(N,1);%initial temp vect (random)
%T0=[1;zeros(N-1,1)];%initial temperature (pt source)
a=ax*[ones(1,50) 0.1 ones(1,49)];%heter. med.
%a=ax*ones(1,N);%homogeneous medium

%operators
lap=-diag([1 2*ones(1,N-2) 1],0)+...
diag(ones(1,N-1),1)+diag(ones(1,N-1),-1);%laplacian
dif=diag([-ones(1,N-1) 0],0)+diag(ones(1,N-1),1);%differ

%initialization
TI=T0;TIB=T0*sqrt(dt);S1=zeros(N,1);S2=zeros(N,1);
S3=zeros(N,1);S4=zeros(N,1);S5=zeros(N,1);

%iteration
for i=2:1000
TIBM=TIB;%noisy field at previous time step

%Forward simulation
t(i)=i*dt;TI=TI+delt*diag(a)*lap*TI+delt*(dif*a).*(dif*TI);
TIB=TIB/sqrt(t(i))+sig*randn(size(TI));%noisy IR signal
Tana=1/2/sqrt(pi*t(i))*exp(-x.*x/4/ax/t(i))*sqrt(t(i));%anal
%plot(x,TIB,x,Tana,'o'),axis([0 N*dx 0 2]), figure(1)
plot(x,TIB),axis([0 N*dx 0 2]), figure(1)

%estimation
S1=S1+(dif*TIBM)*t(i-1)/t(i).*(dif*TIBM);
S2=S2+(lap*TIBM*sqrt(t(i-1)))/t(i).*(TIB*sqrt(t(i))-
TIBM*sqrt(t(i-1)));
S3=S3+(dif*TIBM)*t(i-1)/t(i).*(lap*TIBM);
S4=S4+(dif*TIBM*sqrt(t(i-1)))/t(i).*(TIB*sqrt(t(i))-
TIBM*sqrt(t(i-1)));
S5=S5+(lap*TIBM)*t(i-1)/t(i).*(lap*TIBM);
ae1=(S1.*S2-S3.*S4)/(S1.*S5-S3.*S3);%expression(18)
ae2=S2./S5;%expression(20)

%plotting
plot(x,ae1*dx*dx/dt,x,a),axis(H), figure(2)
plot(x,ae2*dx*dx/dt,x,a), axis(H), figure(3), pause
end
```